

# A practical decoupled stabilizer for joint-position controlled humanoid robots

D. Kaynov\*, P. Souères\*\*, P. Pierro\*, C. Balaguer\*

\*RoboticsLab, University Carlos III of Madrid

dkaynov@ing.uc3m.es, ppierro@ing.uc3m.es, balaguer@ing.uc3m.es

\*\*LAAS-CNRS, University of Toulouse, France

soueres@laas.fr

**Abstract** Efficient methods have so far been proposed for planning dynamically stable walking pattern for humanoid robots. However, to guarantee that the reference joint trajectory will produce a safe movement despite modeling errors and perturbations, a stabilizer needs to be implemented on the robot. Though this stabilizer constitutes an essential part of the control strategy of most advanced humanoid platform, it is usually not open-source and dedicated to the own robot characteristics. The goal of this paper is to propose a general and practical strategy for designing a stabilizer for joint-position controlled humanoid robots. The proposed method is based on a double inverted pendulum model and a decoupling approach thanks to which the position of the ZMP and the center of gravity can be controlled independently through the regulation of the ankle and hip joints. The stabilizer generates the expected stabilizing torques from the admissible joint position input. The resulting control algorithm is fast and can be easily executed on the robot. This algorithm was successfully implemented as real-time plugins for the OpenHRP simulator of the HRP2. Simulations showing the efficiency of the method are presented and discussed.

## I. INTRODUCTION

Inspired by the model of human walking dynamics, different approaches have so far been proposed to control postural stability and locomotion of humanoid robots. Passive dynamic walking schemes were developed to reproduce cyclic energy transformation [1], virtual model control was proposed to introduce compliance into rigid robot dynamics [2], central pattern generator involving nonlinear oscillator was designed for locomotion [3] and hybrid zero dynamics was used for modeling the impact inherent in the dynamics of legged locomotion [4]. However, though these approaches provide interesting adaptive properties, they do not always lead to strongly controllable strategies and therefore cannot be easily applied for driving a robot in a constraint environment where each step need to be precisely positioned.

For this reason, the control of most part of humanoid robots is rather based on the notion of Zero Moment Point (ZMP) [5], [6], [7], [8], from which it is possible to state a simple dynamic-based criterion to guarantee the rotational equilibrium of the robot along planned trajectories. This well-known approach, which allows the design of efficient control algorithms, is based on the measure of the moment of active forces at the contact with the ground. By combining the ZMP approach with the inverted pendulum representation, a clever table-cart dynamic model was

proposed to relate the dynamics of the Center of Gravity (CoG) to the ZMP position [9]. As the control input of most part of humanoid robots is the joint position, the angular variation that allows to move the CoM in order to follow a reference ZMP trajectory can be easily computed from inverse kinematics. An important advantage of this approach is that it does not require the knowledge of a precise model of the robot dynamics, the mass being supposed to be concentrated in one point. However, as the model does not precisely represent the robot – the CoM position being for instance often considered at the center of the pelvis – the walking pattern alone is insufficient to guarantee the walk stability, even on a smooth horizontal floor. As a consequence, a stabilizer turns out to be necessary to maintain a zero error between the values of parameters provided by the walking pattern, and the measured ones. This stabilizer constitutes an essential part of the motion control system of any advanced humanoid robot. For instance, if a dynamically stable walking pattern is sent to the OpenHRP simulator of the humanoid robot HRP2 [13], while its stabilizer is inactivated, the robot loses rapidly its balance. However, though the stabilizer constitutes an essential part of the motion control system, it is usually not open-source. This regulation loop is then likely to be closely dependent on the own robot characteristics and, as a consequence, not described as a general algorithm that could be applied to other humanoid platforms.

The goal of this paper is to propose a simple and practical strategy for designing a stabilizer for joint-position controlled humanoid robots. The proposed method is based on a model of double inverted pendulum and a decoupling approach, thanks to which the ZMP and the CoG position errors can be regulated by controlling the ankle and hip joints independently. The controller allows to generate the stabilizing torques from the admissible joint position input. The resulting control algorithm is fast and can be easily executed on the robot. It was successfully implemented as real-time plugins for the OpenHRP simulator of HRP2. Simulations showing the efficiency of the method will be presented and discussed.

The paper is organized as follows: Section II recalls basic concepts related to the problem of humanoid robot's stability. The double inverted pendulum model, which is used for the stabilization control, is presented in section III. Section IV describes the decoupled control strategy. Section V presents the implementation of the stabilizer on the OpenHRP simulator and provides experimental results and

discussion. The conclusion is given in section VI

## II. STABILIZATION CONTROL

An efficient approach to produce a stable bipedal locomotion for humanoid robots is to determine a secure motion pattern for each joint by using the table-cart state space representation proposed in [9], which combines the 3D linear Inverted Pendulum dynamics (3D-LIPM) [10], [11] and the ZMP criterion [5][6][12]. Under the hypothesis that the CoG remains within the horizontal plane of altitude  $z_c$ , the ZMP coordinates,  $(x_{ZMP}, y_{ZMP})$  can be expressed as functions of the CoG position  $(x, y)$  and acceleration as follows:

$$x_{ZMP} = x - \frac{z_c}{g} \ddot{x} \quad (1)$$

$$y_{ZMP} = y - \frac{z_c}{g} \ddot{y} \quad (2)$$

Using this relation, different motion generation algorithms were proposed in [8], [9], [11], and many other recent publications. The basic idea is to control the CoG in order to guarantee that the ZMP position will follow a prescribed safe trajectory. This is done through the computation of inverse kinematics which allows determine the appropriate joint displacement. The reference ZMP trajectory is usually constructed by interpolating the successive foot placements. However, as the inverted pendulum model does not fully capture the robot dynamics, this control scheme cannot be sent in open-loop to the robot. A stabilizer appears then to be necessary to guarantee a good tracking of the reference trajectory. This is precisely the problem which is addressed in this paper.

According to the previous reasoning, two important variables are to be considered: The ZMP error  $e_{ZMP}$  and the CoG error  $e_{COG}$ , respectively defined by:

$$e_{ZMP} = ZMP^d - ZMP^a \quad (3)$$

$$e_{COG} = COG^d - COG^a \quad (4)$$

where the superscript “ $d$ ” and “ $a$ ” respectively stand for the desired and actual positions

The ZMP controller should implement a strategy for moving the actual ZMP to the desired value. An easy way to proceed is to control the ankle joint by considering the part of the robot located above this joint as a solid. However, though the proposed compensational mechanism allows to displace the actual ZMP position, it introduces new errors. Indeed, when the upper body is rotated with respect to the ankle joint, body angle errors  $\Delta q_{Bf}(t)$  and  $\Delta q_{Bs}(t)$  appear in the frontal and sagittal planes respectively, as shown in figure 1.

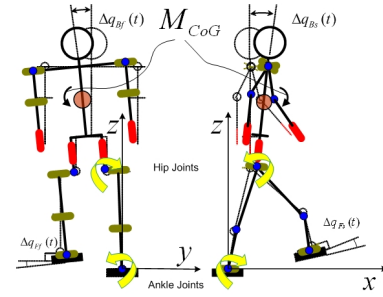


Fig. 1: Errors compensation

These errors generate tilting moment  $M_{CoG}$  and angle errors,  $\Delta q_{Ff}(t)$  and  $\Delta q_{Fs}(t)$ , in the sagittal and frontal planes respectively, during the positioning of the hanging foot. This effect may introduce strong instability and vibrations when the foot is landing, and can overturn the robot. The tilting moment  $M_{CoG}$  should be compensated by the Attitude control algorithm which tries to maintain the trunk of the robot strictly vertical in every stage of its motion, thus, eliminating the tilting moment and body inclination errors.

The most effective way to control the body inclination is to maintain its backbone strictly vertical during all the movement. In this case, it is sufficient to control the hip joints in the frontal and sagittal planes (figure 1). Finally, note that research works in biomechanics have also pointed out the role of hip and ankle in balance control [14].

## III. DOUBLE INVERTED PENDULUM

As explained in the preceding section, the objective is to design a stabilizer to regulate simultaneously the ZMP and the attitude position by acting on the ankle and hip joints respectively. To this end, an interesting model is to consider the humanoid robot, in the sagittal and the frontal plane, as an inverted double pendulum, as illustrated in figure 2.

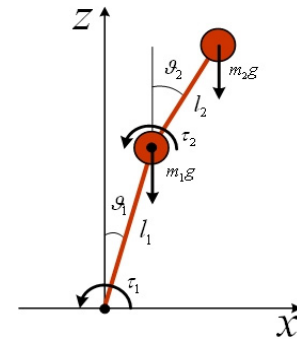


Fig. 2: Humanoid robot modeling as a double inverted pendulum

In each of these two vertical planes, consider a double bob pendulum with masses  $m_1$  and  $m_2$  attached by rigid massless links of lengths  $l_1$  and  $l_2$ . Let us denote by  $m = m_1 + m_2$  the total mass of the robot. The posture of the robot is defined by the angles  $\vartheta_1$  (ankle joint) and  $\vartheta_2$  (hip joint) with respect to the vertical. Considering this representation, the potential energy of the system is given by

$$V = (m_1 + m_2)gl_1 \cos \vartheta_1 + m_2gl_2 \cos \vartheta_2 \quad (5)$$

whereas its kinetic energy is :

$$T = \frac{1}{2}m_1l_1^2\dot{\vartheta}_1^2 + \frac{1}{2}m_2[l_1^2\dot{\vartheta}_1^2 + l_2^2\dot{\vartheta}_2^2 + 2l_1l_2\dot{\vartheta}_1\dot{\vartheta}_2 \cos(\vartheta_1 - \vartheta_2)] \quad (6)$$

By expressing the Lagrangian  $H=T-V$  from (5) and (6), applying the Euler Lagrange equation, and considering only small variations of angles  $\vartheta_1$  and  $\vartheta_2$  the system dynamics can be well approximated by the following linearized model, in which terms of second order and higher have been neglected:

$$(m_1 + m_2)l_1^2\ddot{\vartheta}_1 + m_2l_1l_2\ddot{\vartheta}_2 - l_1g(m_1 + m_2)\vartheta_1 = \tau_1 \quad (7)$$

$$m_2l_2^2\ddot{\vartheta}_2 + m_2l_1l_2\ddot{\vartheta}_1 - l_2m_2g\vartheta_2 = \tau_2 \quad (8)$$

Different control schemes can be used to stabilize the system (7), (8). The strategy considered in this paper is based on a decoupling property of the system, which is described in the next section.

#### IV. DECOUPLED CONTROL

##### A. Decoupling the dynamics

Though different linear control techniques can be used to stabilize directly the system described by equations (7) and (8), in practice these approaches have some inconveniences. The main problem comes from the fact that this model considers control torques of both the hip and ankle joints as input, whereas most of contemporary humanoid robots are driven by DC motors with position control. To cope with this problem we propose a decoupled approach for the control of the ZMP and the CoG, which was suggested by the analysis of the closed-loop dynamics of the double inverted pendulum. Figure 3 shows the evolution of the joint angles  $\vartheta_1$  and  $\vartheta_2$  for various initial conditions, that can be interpreted as different perturbations acting on the robot.

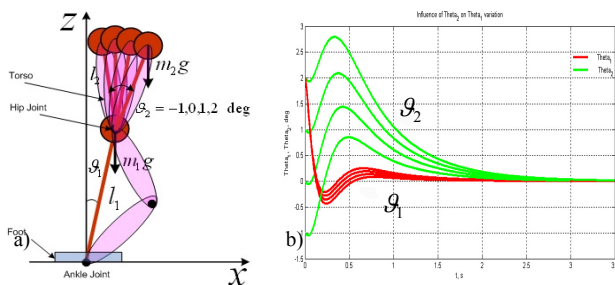


Fig. 3: a) Variation of  $\vartheta_2$  on the model, b) Influence of  $\vartheta_2$  on  $\vartheta_1$ .

As represented in figure 3(b), large variations of  $\vartheta_2$  have no significant influence on the dynamics of  $\vartheta_1$ . Indeed, the time response of  $\vartheta_1$  remains practically identical for various initial values of  $\vartheta_2$ . On the other hand, the variation of  $\vartheta_1$  can be considered as a perturbation on the dynamics of  $\vartheta_2$ , that will be compensated by the controller. In other words,

ankle's joint variation (ZMP control) affects more the attitude position than hip's variation (Attitude control) affects the ZMP. Therefore, the attitude control should be faster in order to compensate disturbances brought by the ankle variation. In order to determine how much faster the control of the upper pendulum ( $\vartheta_2$ ) should be in order to compensate all possible perturbations caused by the motion of the bottom pendulum ( $\vartheta_1$ ), let us consider both dynamics in terms of their natural frequency:

$$\frac{\omega_{n2}}{\omega_{n1}} = \sqrt{\frac{l_1}{l_2}} \quad (9)$$

Thus, taking for example  $l_1 = 1.2 \text{ m}$ ;  $l_2 = 0.2 \text{ m}$ , the control of the upper pendulum should be at least 2.45 times faster in order to compensate the dynamics of the bottom. Taking into account this consideration, the stabilizer can be considered as a sum of two decoupled components devoted to Attitude control ( $\vartheta_2$ ) and ZMP control ( $\vartheta_1$ ).

Therefore, the second order nonlinear coupled differential equations (7), (8) describing the dynamics of the double inverted pendulum can be transformed into the following two decoupled dynamical equations:

$$(m_1 + m_2)l_1^2\ddot{\vartheta}_1 - l_1(m_1 + m_2)g\vartheta_1 = \tau_1 \quad (10)$$

$$m_2l_2^2\ddot{\vartheta}_2 - l_2m_2g\vartheta_2 = \tau_2 \quad (11)$$

Equations (10) and (11) express the dynamical equations of single inverted pendulums.

##### B. ZMP control

By replacing  $(m_1+m_2)$  in equation (10) by the total mass  $m$  located at the CoG we obtain:

$$\tau_1 = ml_1^2\ddot{\vartheta}_1 - gml_1\vartheta_1 \quad (12)$$

where  $\tau_1$  is the torque generated at the ankle joint,  $\vartheta_1$  its angular position and  $l_1$  distance between the joint and the CoG. The main difficulty comes from the fact that equation (12) is not well appropriate for designing of a ZMP control scheme with the ankle joint position as input. To this end, the model needs to be slightly completed in order to take into account the existing compliance at the ankle joint. Thanks to this compliance, the robot exhibits the characteristics of a lightly damped structure [15]. The most suitable model in this case is a single mass inverted pendulum with compliant joint, as presented in figure 4, where  $u$  denotes the desired ankle joint angle,  $\vartheta_1$  is the actual pendulum angle,  $K$  denotes the joint stiffness, and  $\tau_1$  is the torque produced by the motor.

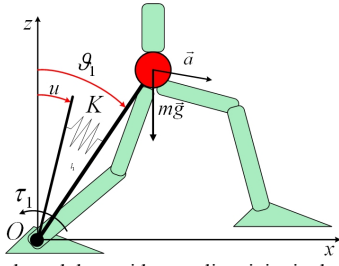


Fig. 4: Inverted pendulum with compliant joint in the sagittal plane

Neglecting the existence of the damping in the system, the equation describing a spring torque has the form:

$$\tau_1 = K(\vartheta_1 - u) \quad (13)$$

On the other hand, from the equation relating the moment produced by the ground reaction force around the  $y$  axis with  $x$  ZMP direction (the planar  $XZ$  case of the inverted pendulum is considered) we get:

$$\tau_y = -mgx_{ZMP} \quad (14)$$

For the static equilibrium of the system, the moment generated by the motor at the ankle joint should compensate the moment produced by the ground reaction force. By identifying the expression of  $\tau_1$  in equations (12) and (13) we get the following relation:

$$ml_1^2 \ddot{\vartheta}_1 - mgl_1 \vartheta_1 = K(\vartheta_1 - u) \quad (15)$$

Introducing the state variables  $x_1 = -\frac{ml_1^2}{K} \vartheta_1$  and  $x_2 = \dot{x}_1$ , equation (15) can be rewritten as 2<sup>nd</sup> order linear system with  $u$  as control input as follows:

$$\begin{bmatrix} \dot{x}_1 \\ \dot{x}_2 \end{bmatrix} = \begin{bmatrix} 0 & 1 \\ \frac{K + mgl_1}{ml_1^2} & 0 \end{bmatrix} \begin{bmatrix} x_1 \\ x_2 \end{bmatrix} + \begin{bmatrix} 0 \\ 1 \end{bmatrix} u \quad (16)$$

The expression of the output  $x_{ZMP}$  is obtained by equating relations (13) and (14) which, in terms of the state variables  $x_1$  and  $x_2$ , writes:

$$x_{ZMP} = \begin{bmatrix} \frac{K^2}{m^2 l_1^2 g} & 0 \end{bmatrix} \begin{bmatrix} x_1 \\ x_2 \end{bmatrix} + \frac{K}{mg} u \quad (17)$$

The state space representation (16), (17) is under controllable canonical form. On this basis, a LQR controller can be easily designed to keep the actual ZMP close to its reference position. Finally, it should be mentioned that ZMP control in the frontal  $YZ$  plane can be treated in the same way. The whole humanoid can be interpreted as a combination of two planar inverted pendulums, in frontal and sagittal planes, controlled by four independent ankle joints.

### C. Attitude control

Recall that the aim of the attitude control is to maintain the trunk of the humanoid robot in vertical position. As for

the ZMP control, the decoupling strategy allows to consider the model of a single inverted pendulum. In that case, there is no need for introducing compliance as the hip joint. As the supported mass is less important, the trunk can be considered as rigid. The dynamical model of the inverted pendulum is expressed by equation (11), in which  $\tau_2$  is the torque applied at the hip joint that allows control the upper body orientation  $\vartheta_2$ ,  $l_2$  is the distance from the hip joint to the point where the mass  $m_2$  of the upper body is concentrated (figure 5).

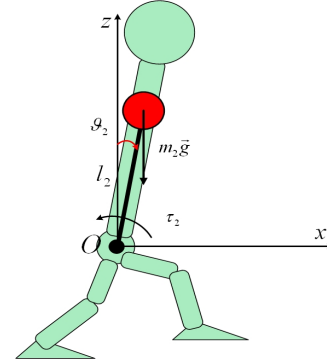


Fig. 5: Simple inverted pendulum

A simple proportional controller appears then sufficient to regulate the pendulum in vertical position ( $\vartheta_2 = 0$ ). The developed controller can be understood as an additional position regulator functioning over the standard hip joint position controller. The controller's output is the correction for the actual hip joint position:

$$\Delta \vartheta_H(t) = K_p e(t) \quad (18)$$

where  $K_p$  is a proportional gain which can be tuned experimentally and  $e(t)$  is the upper body orientation error with respect to the vertical direction provided by the inertial central unit. To conclude, it should be mentioned that the actual 3D trunk's motion can be interpreted as a combination of two planar inverted pendulums in frontal and sagittal planes which have practically the same dynamics.

### D. General Stabilizer Architecture

The overall control architecture including the parts presented in the preceding sections is described in figure 6.

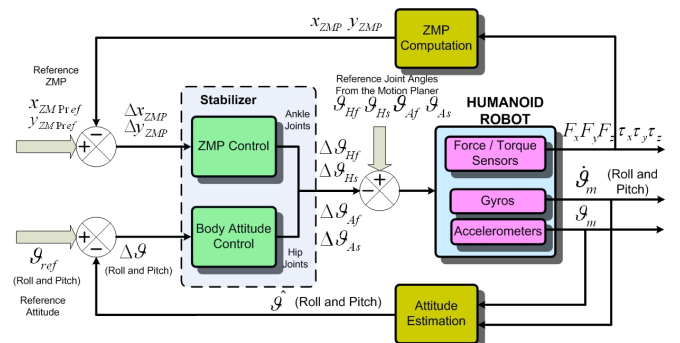


Fig. 6: Stabilizer architecture

The force sensor system of the robot consisting of two six-axis force-torque provides the controller with the real distribution of the forces and torques  $F_x, F_y, F_z, \tau_x, \tau_y, \tau_z$  at the contact between the foot and the ground. The 3-axis Gyro and Accelerometer provide the measurements of the angular position  $\mathcal{G}_m$  and angular velocity  $\dot{\mathcal{G}}_m$  of the upper body (trunk) of the robot in the frontal and sagittal planes (Roll and Pitch). After the actual ZMP position  $x_{ZMP}, y_{ZMP}$  is computed by the ZMP Computational module, and the real attitude is estimated by the Attitude Estimation module, the ZMP error  $\Delta x_{ZMP}, \Delta y_{ZMP}$  and the attitude error  $\Delta \mathcal{G}$  can be estimated [16]. These errors are the input data for the decoupled stabilizer which regulates the ZMP and attitude positions by controlling the ankle and hip joints. Finally, the compensational motion of the ankle  $\Delta \mathcal{G}_{Af}, \Delta \mathcal{G}_{As}$  and hip  $\Delta \mathcal{G}_{Hf}, \Delta \mathcal{G}_{Hs}$  joints in the frontal and sagittal planes are added to the desired values of angles  $\mathcal{G}_{Af}, \mathcal{G}_{As}, \mathcal{G}_{Hf}, \mathcal{G}_{Hs}$  given by the motion pattern generator. The implementation of the decoupled stabilizer provides fast and easy control of the walking stability. All changes are applied to ankle and hip joints eliminating the need of inverse kinematics computation.

## V. SIMULATIONS AND DISCUSSION

Several tests were done on the OpenHRP simulator which implements an accurate model of the dynamics of HRP2. In order to test the functioning of the stabilizer in static (non-walking) position, the robot was exposed to external disturbances. Both parts of the stabilizer (ZMP and attitude controls) were tested independently. In order to test the attitude control, a disturbing force  $F_d$  was applied to the lower part of the humanoid's body. This force was simulated by a motion of the ankle (Figure 7(a)). In a similar way, to test the ZMP control, a disturbing force was applied to the upper part of the robot. This force was simulated by a hip movement (Figure 7(b)). In both cases, the excitation was realized as a sinusoidal movement of amplitude  $5^\circ$  for the attitude control, and  $3^\circ$  for the ZMP control.

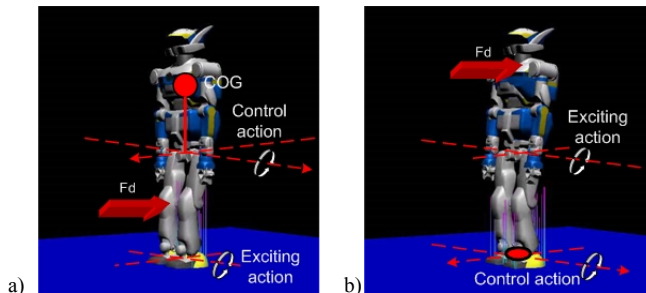


Fig. 7: Static test of the stabilizer in the sagittal plane a) attitude control b) ZMP control

The results of static tests of the Attitude and ZMP controllers on the dynamic model of HRP2 are shown in

figures 8 and 9 respectively.

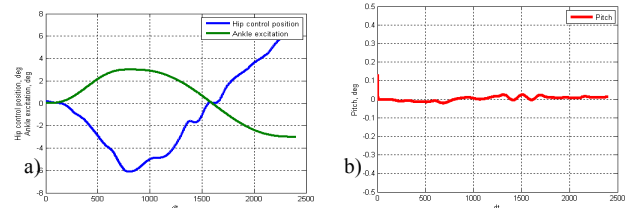


Fig. 8: Static test for Attitude control a) Hip control position and Ankle excitation variation b) Pitch variation

It appears clearly in the figure 8 that the variation of the pitch angle of the trunk is minimal (less than  $0.02$  deg), showing that the upper part is maintained almost vertical.

Under the ankle control (figure 9), the ZMP variation appears rather smooth. In the final phase, the ZMP is perturbed but rapidly stabilized.

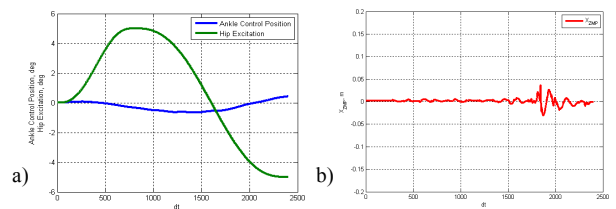


Fig. 9: Static test for ZMP control a) Ankle control position and Hip excitation variation b)  $x_{ZMP}$  variation.

Figure 10 presents a sequence of snapshots during the simulation of a walking trajectory with the proposed stabilizer.

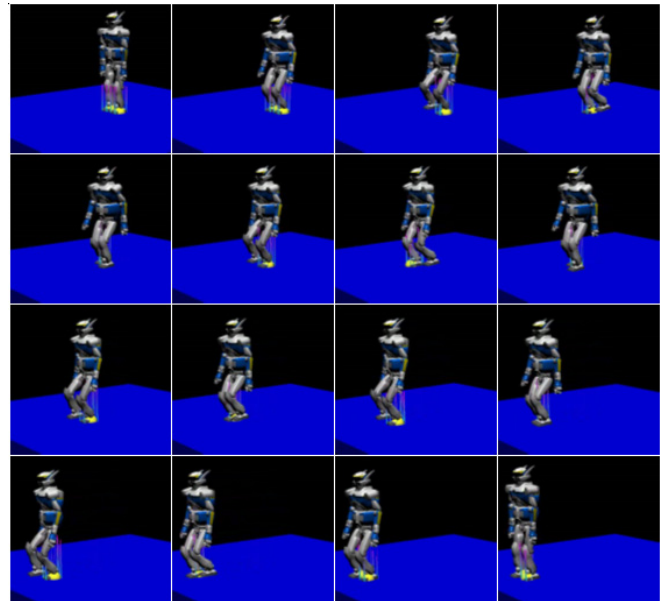


Fig. 10: Snapshots of humanoid simulator. Walking with designed stabilizer.

As in the previous test, the robot starts from the initial vertical position. First, it takes the half-sitting posture. Following this stage, the walk starts. The robot executes 10 steps to cover a distance of 2 m. After the goal was reached, the robot gets back to the initial vertical posture. During this walking test the balance is perfectly maintained, showing the

efficiency of the stabilizer.

Figure 11 shows the variation of the ZMP coordinates in each plane (sagittal and frontal) during the walk. The actual ZMP (measured by the force-torque sensors) is superposed to the planned one. The periodicity of ZMP curves is due to the cycle of steps.

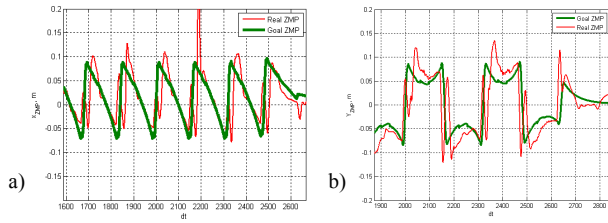


Fig. 11: Reference and real ZMP variation a)  $x_{ZMP}$  b)  $y_{ZMP}$

Both ZMP components oscillate near the reference values, however some peaks (in worst cases the ZMP even leaves the stability zone) can be observed. Nevertheless, as shown by the experiments, the robot balance is maintained. This can be related to the fact that the OpenHRP simulator does not always compute the true ZMP. In the simulator, the foot mass exists under the ankle force sensor. When the sole instantaneously leaves the floor, its acceleration generates a pulling force that produces a wrong ZMP value, which escapes the stability zone. The ZMP error depends on the tuning of the ZMP controller. As mentioned above, a lower priority was given to the ZMP control to introduce minimum disturbance in the ankle motion. Figure 12 presents the attitude variation. The trunk of the humanoid robot is maintained vertical (zero pitch and yaw). Peaks in both curves are due to foot impact with the ground and never exceed  $1^\circ$ .

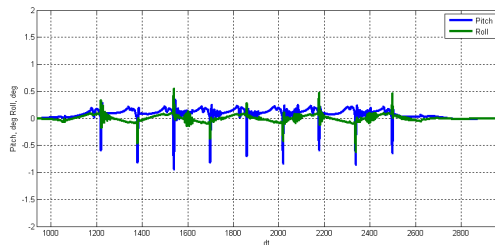


Fig. 12. Attitude variation

## VI. CONCLUSION

Though “dynamically stable” walking patterns can be deduced from 3D-LIPM and ZMP-based approaches, their implementation on a humanoid platform requires a closed-loop stabilizer to cope with modelling errors and perturbations. To this end, we proposed a generic and practical stabilizer, which provides online modification of the motion pattern to guarantee walking stability. The ZMP and CoG positions were shown to be the key variables that need to be adjusted by the stabilizer. The most effective way to correct the ZMP position is to modify the trajectory of the supporting ankle joint, whereas the best way to control the position of the COG is to regulate the attitude of the upper body by acting on the hip joint. Introducing a double

inverted pendulum model, we had shown that both variables can be simultaneously controlled, thanks to a decoupling approach. Using an appropriate convergence rate, we proved that the influence of each variable on the other becomes negligible. On this basis, a closed-loop compensatory scheme was designed to update the walking pattern in real-time. The main advantage of the method is to allow fast online correction of the posture, without requiring the computation a new walking gait or inverse kinematics. Numerous tests on the OpenHRP simulator of HRP2 have proven the efficiency of the approach. Finally, though most advanced humanoid platform include stabilizers, which are unfortunately not open-source, we provide here a general and practical control scheme for joint-position controlled humanoid robot.

## REFERENCES

- [1] T. McGeer. “Passive Dynamic Walking.” *International Journal of Robotics Research*. Vol. 9, pp. 62-82, 1990
- [2] J. Pratt, P. Dilworth, and G. Pratt, “Virtual Model Control of a Bipedal Walking Robot”, *IEEE Int. Conference on Robotics and Automation*, Albuquerque, New Mexico, USA, 1997.
- [3] K. Tsuchiya, S. Aoi, K. Tsujita, “Locomotion control of Biped Locomotion Robot using Nonlinear Oscillators”, *IEEE Int. Conf. on Intelligent Robots and Syst.*, Las Vegas, Nevada, USA, 2003
- [4] E.R. Westervelt, J.W. Grizzle, D.E. Koditschek, “Hybrid Zero Dynamics of Planar Biped Walkers, *IEEE Transaction. on Automatic Control*, 48 (1) pp 42-56, 2003.
- [5] M. Vukobratovic, A. A. Frank, and D. Juricic, “On the stability of biped locomotion,” *IEEE Transactions on Biomedical Engineering*, pp. 25–36, January 1970.
- [6] K. Hirai, M. Hirose, Y. Haikawa, and T. Takaneda, “The development of Honda Humanoid Robot”, *IEEE Int. Conference on Robotics and Automation*, Leuven Belgium, 1998.
- [7] F. Pfeiffer, K. Löffler, and M. Gienger, “The concept of Jogging Johnie”, *IEEE Int. Conference on Robotics and Automation*, Washington DC, USA, 2002.
- [8] E. Yoshida, O. Kanoun, C. Esteves and J-P. Laumond. “Task-driven Support Polygon Humanoids”. *IEEE-RAS Int. Conference on Humanoid Robots*, Genova, Italy, 2006.
- [9] S. Kajita, F. Kanehiro, K. Kaneko, K. Fujiwara, K. Harada, K. Yokoi, and H. Hirukawa, “Biped walking pattern generation by using preview control of zero-moment point,” *IEEE Int. Conference on Robotics and Automation*, Taipei, Taiwan, 2003.
- [10] S. Kajita, F. Kanehiro, K. Kaneko, K. Yokoi and H. Hirukawa, “The 3D Linear Inverted Pendulum Mode: A simple modeling for a biped walking pattern generation”. *In Proc. IEEE Conf on Intelligent Robots and Systems (IROS 2001)*, pp. 239-246, Hawaii, 2001.
- [11] T. Sughiara, Y. Nakamura, and H. Inoue, “Realtime Humanoid Motion Generation through ZMP manipulation based on Inverted Pendulum Control,” *IEEE Int. Conf. on Robotics and Automation*, Washington DC, USA, 2002
- [12] S. Kagami, T. Kitagawa, K. Nishiwaki, T. Sughiara, M. Inaba, and H. Inoue, “A Fast Dynamically Equilibrated Walking Trajectory Generation Method of Humanoid Robot”, *Autonomous Robots*, 12, 71-82, 2002.
- [13] K. Kaneko, et al., “The Humanoid Robot HRP-2”, *IEEE/RSJ Int. Conf. on Robotics and Automation*, 1083-1090, 2004.
- [14] A. Kuo, “An optimal control model for analyzing human postural balance,” *IEEE Transactions on Biomedical Engineering*, vol. 42, no. 1, pp. 87–101, January 1995.
- [15] J. Kim and J. Oh, Walking Control of the Humanoid Platform KHR-1 based on Torque Feedback Control, *Proc. of IEEE Intl. Conf. on Robotics and Automation*, pp. 623-628, 2004.
- [16] K. Löffler, M. Gienger, F. Pfeiffer, Sensors and Control Concept of a Biped Robot, *IEEE Transactions on Industrial Electronics*, vol. 51, 2004.